Influence of geminate recombination kinetics on the shape of low field MARY line

Yu.V. Toropov [a], F.B. Sviridenko [b], D.V. Stass [a,b], A.B. Doktorov [a,b], Yu.N. Molin [a,b,*]

[a] *Novosibirsk State University, 630090 Novosibirsk, Russian Federation*
[b] *Institute of Chemical Kinetics and Combustion, 630090 Novosibirsk, Russian Federation*

Abstract

The influence of diffusional kinetics of geminate recombination of radical ion pairs on the shape of MAgnetic field dependence of Reaction Yield (MARY) spectra in weak magnetic fields is analysed in some detail. It is shown that the low-field line is not Lorentzian and has broader wings and a sharper peak. The deviation from the Lorentzian shape is most clear when the times of spin relaxation and chemical transformation of radical ions are much longer than the characteristic time scale of the geminate recombination. Under this condition, the full width at half magnitude is related primarily to the recombination time, whereas the width between the points of maximum slopes is determined by spin relaxation and chemical decay. The low-field MARY line was analysed for the pairs $(n\text{-alkane})^+/C_6F_6^-$. It was found that the line shape is indeed not Lorentzian, and is well described by the suggested theory. © 2000 Elsevier Science B.V. All rights reserved.

1. Introduction

Magnetic field dependence of the reaction yield (MARY spectrum) in the recombination of long-lived spin-correlated radical pairs often demonstrates sharp features (lines) in the vicinity of zero field [1–12] and in characteristic fields of the order of hyperfine couplings within the pair [8–12], where the spin terms are degenerate. It has also been suggested that a similar effect may appear in high magnetic fields for radicals with nonequal *g*-factors [13]. The feature in low fields has an ex-

tremum at zero magnetic field and, to make it look like a line, magnetic field is often swept through zero, going from "negative" to "positive" values, and the resulting line is often referred to as the "Zero field line". Its width depends on the lifetime of the coherent spin state of the pair, which is determined by spin relaxation and chemical transformations of the radical partners [14]. The line is usually observed on the background of the ordinary magnetic field effect coming from the interplay of Zeeman and hyperfine interactions within the radical pair [15]. If the line width is small compared to the average hyperfine coupling in the radical pair (approximation of the "isolated" line) and recombination kinetics of the pair is exponential, then the shape of the line is Lorentzian and the lifetime of the spin correlated pair can be easily extracted from the line width. Such

---
* Corresponding author. Address: Institute of Chemical Kinetics and Combustion, 630090 Novosibirsk, Russian Federation. Tel.: +7-3832-331607; fax: +7-3832-342350.
  E-mail address: molin@ns.kinetics.nsc.ru (Y.N. Molin).

an approach was recently used to estimate chemical stability of solvent radical cations (holes) in liquid *n*-alkanes [16].

However, there is some evidence that in low fields, the shape of MARY line may differ from the Lorentzian one [11]. A possible reason for such a deviation is the diffusional character of recombination kinetics in liquid solution, which results in nonexponential distribution of recombination times of radical pairs.

In this paper, we analyse the influence of the recombination kinetics on the shape of MARY line. Without any loss of generality, it is assumed that the MARY spectra are recorded by sampling the delayed fluorescence from radical ion pairs initially formed in a singlet state.

2. Theory

2.1. Magnetic field effect

Magnetic field effect (MARY spectrum) $F(H)$ is the dependence of the quantum yield of the delayed fluorescence from the singlet state of the radical ion pair on the magnetic field H and for the spin-independent recombination is given by

$$F(H) \propto \int_0^\infty \rho_{SS}(t) f(t) \, dt$$
$$\equiv \int_0^\infty \rho_{SS}^D(t) e^{-t/T} f(t) \, dt. \tag{1}$$

Here $\rho_{SS}(t)$ is the population of the singlet state of the radical ion pair at a given time t. Function $f(t)$ is the lifetime distribution of the geminate radical ion pairs. The singlet state population is determined by the spin dynamics $\rho_{SS}^D(t)$ and by the irreversible processes, such as chemical transformations of the constituent radical ions and their spin relaxation. In the case when the rate of chemical decay is also spin-independent (the only case considered in this article), it may be accounted for using a multiplicative factor $e^{-t/T}$, where T is the natural lifetime of radical ions. Spin relaxation within radicals can be accounted for in a similar way. As a reasonable approximation, a single relaxation time can be used since the pair

partners make an additive contribution to the spin coherence decay [17] and T_1 and T_2 are approximately equal in the vicinity of zero magnetic field.

2.2. Spin evolution of geminate radical ion pairs

Spin evolution of a radical ion pair depends on the configuration of magnetic nuclei in radical ions. Consider a pair in which one of the radicals has no magnetic nuclei while the other has n equivalent spin-1/2 nuclei, the g-factors of both radicals being equal. Dividing the pairs into subensembles with total nuclear spin I, the problem can be reduced to the description of a pair having one spin-I nucleus, and the spin evolution may be found by subsequent averaging over the distribution of the possible values of I. Therefore, we will examine a single nucleus pair, for which [15]:

$$\rho_{SS}^D(t) = \frac{1}{4(2I+1)} \sum_{m=-I}^{I} |e^{-i\omega t}(e^{-iR_m t} \cos^2 \varphi_m$$
$$+ e^{-iR_m t} \sin^2 \varphi_m) + e^{-iR_{m-1} t} \sin^2 \varphi_{m-1}$$
$$+ e^{-iR_{m-1} t} \cos^2 \varphi_{m-1})|^2, \tag{2}$$

where

$$R_m = \tfrac{1}{2}(\omega^2 + (2m+1)a\omega + a^2(I + \tfrac{1}{2})^2)^{1/2},$$

$$\cos^2 \varphi_m = \frac{1}{2R_m} \left(R_m + \frac{\omega}{2} + \frac{a}{2} \left(m + \frac{1}{2} \right) \right), \tag{3}$$

here

$$\omega = g\beta H/\hbar, \tag{4}$$

where g is the g-factor of radical ions, β is the Bohr magneton, H is the external magnetic field and a is the hyperfine coupling constant (in the frequency units). The sum in Eq. (2) runs over all possible values of nuclear spin projection m.

Substituting Eq. (2) into Eq. (1) gives the field dependence $F(H)$ of the singlet product yield for a radical ion pair with a given nuclear spin I. Let us examine the isolated line centered at zero magnetic field. Spin dynamics corresponding to this line can be extracted from Eq. (2) by taking the limit $a \to \infty$. It is then assumed that integration over time nullifies all the terms oscillating with frequencies depending on a.

In this approximation, Eq. (2) yields two oscillating terms

$$\rho_{SS}^{D}(t) = \frac{1}{6(2I+1)^2} \left\{ 8I(I+1) + 3 + (2I+3)(I+1) \right.$$
$$\times \cos \frac{2I}{2I+1} \omega t + I(2I-1)$$
$$\left. \times \cos \frac{2(I+1)}{2I+1} \omega t \right\}.$$
$$(5)$$

For $I = 1/2$

$$\rho_{SS}^{D}(t) = \frac{1}{4} \left(\frac{3}{2} + \cos \frac{\omega t}{2} \right) \tag{6}$$

while for $I \to \infty$

$$\rho_{SS}^{D}(t) = \frac{1}{6}(2 + \cos \omega t). \tag{7}$$

The only important difference between Eqs. (6) and (7) is the factor of two in the frequency of spin nutation in a given magnetic field. This means that the low-field MARY line for $I \to \infty$ is two times narrower than the line for $I = 1/2$.

2.3. Lifetime distribution function $f(t)$

Distribution $f(t)$ of recombination lifetimes depends on the initial distribution of the radical ion partners, their diffusional mobility, the solvent polarity, etc. Let us investigate how the shape of the low-field MARY line depends on $f(t)$. To check this we examine the following functions:

$$f_1(t) = \sqrt{\frac{\lambda}{\pi t}} - \lambda \exp(\lambda t) \operatorname{erfc}(\sqrt{\lambda t}), \tag{8a}$$

$$f_2(t) = \frac{1}{\sqrt{\pi \lambda} t^{3/2}} \exp\left(-\frac{1}{\lambda t}\right), \tag{8b}$$

$$f_3(t) = \frac{1}{2} \frac{\lambda}{(1+\lambda t)^{3/2}}, \tag{8c}$$

where $\operatorname{erfc}(x)$ is the complementary probability integral. Fig. 1 shows a plot of the dimensionless distributions $(1/\lambda)f_i(t)$ $(i = 1, 2, 3)$ with respect to dimensionless parameter λt.

The common feature of all these distributions is their asymptotic behaviour $f(t) \sim t^{-3/2}$ for longer
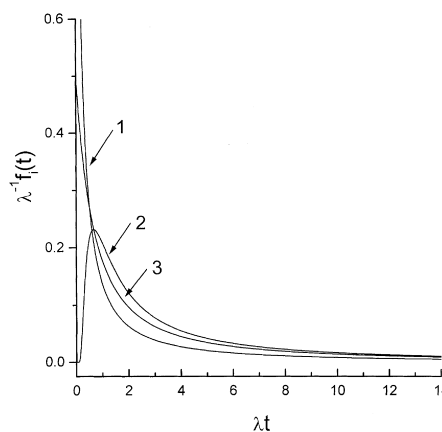

Fig. 1. Model distribution functions over recombination lifetimes of radical ion pairs used for calculations (see Eqs. (8)). The plot shows dimensionless distributions $(1/\lambda)f_i(t)$ $(i = 1, 2, 3)$ versus dimensionless parameter λt for $1 - f_1(t)$, $2 - f_2(t)$ and $3 - f_3(t)$.

times that corresponds to the diffusional motion of radical ions separated by a large distance. Function $f_1(t)$ was suggested [18] to simulate recombination of $e^-/(alkane)^+$ pairs in irradiated alkanes. This will be examined in more detail. Two other functions were chosen to modify the short-time behaviour. While the first function diverges as $t^{-1/2}$ at $t \to 0$, the second tends to zero, and the third monotonously reaches a finite nonzero value.

2.4. The shape of the low field line

Substituting Eq. (5) into Eq. (1) gives the magnetic field effect curves $F_i(\omega)$ in the vicinity of the zero field for different distribution functions $f_i(t)(i = 1, 2, 3)$ over lifetimes of radical ion pairs. Subtracting from the curve the field independent term one can represent the final result as follows:

$$\eta_i(\omega) \equiv F_i(\omega) - \frac{8I(I+1)+3}{6(2I+1)^2} L_i(0)$$
$$= \frac{1}{6(2I+1)^2} \left\{ (2I+3)(I+1)L_i\left(\frac{2I}{2I+1}\omega\right). \right.$$
$$\left. + I(2I-1)L_i\left(\frac{2(I+1)}{2I+1}\omega\right) \right\},$$
$$(9)$$

where

$$L_i(v) = \int_0^\infty \cos(vt)\exp\left(-\frac{t}{T}\right)f_i(t)\,dt. \qquad (10)$$

Function $\eta_i(\omega)$ which satisfies the condition

$$\lim_{\omega\to\pm\infty}\eta_i(\omega) = 0 \qquad (11)$$

describes the shape of the line.

Using distributions (8) one obtains from Eq. (10)

$$L_1(v) = \frac{\lambda T(\lambda T - 1)}{(\lambda T - 1)^2 + v^2 T^2} - \sqrt{\frac{\lambda T}{2}}$$
$$\times \frac{(\lambda T - \sqrt{1+v^2 T^2})}{(\lambda T - 1)^2 + v^2 T^2}$$
$$\times \sqrt{1+\sqrt{1+v^2 T^2}}, \qquad (12a)$$

$$L_2(v) = \cos\left(\sqrt{\frac{2(\sqrt{1+v^2 T^2}-1)}{\lambda T}}\right)$$
$$\times \exp\left(-\sqrt{\frac{2(\sqrt{1+v^2 T^2}+1)}{\lambda T}}\right), \qquad (12b)$$

$$L_3(v) = 1 - \sqrt{\frac{\pi}{\lambda T}}\,\mathrm{Re}\sqrt{1+i|v|T}\exp\left(\frac{1+i|v|T}{\lambda T}\right)$$
$$\times \mathrm{erfc}\left(\sqrt{\frac{1+i|v|T}{\lambda T}}\right) \qquad . \qquad (12c)$$

In the forthcoming discussion, we will refer to $L_i(v)(i=1,2,3)$ when talking about the shape of the spectral line.

Let us first investigate the behaviour of these functions for $T\to\infty$, when the line shape is determined by geminate recombination only. From Eqs. (12a)–(12c) at $T\to\infty$ one obtains

$$L_1(v) = \frac{1}{1+\frac{v^2}{\lambda^2}}\left(1 - \sqrt{\frac{|v|}{2\lambda}}\left(1 - \frac{|v|}{\lambda}\right)\right), \qquad (13a)$$

$$L_2(v) = \cos\left(\sqrt{\frac{2|v|}{\lambda}}\right)\exp\left(-\sqrt{\frac{2|v|}{\lambda}}\right), \qquad (13b)$$

$$L_3(v) = 1 - \sqrt{\frac{\pi|v|}{\lambda}}\mathrm{Re}\sqrt{i}\exp\left(i\frac{|v|}{\lambda}\right)\mathrm{erfc}\left(\sqrt{i\frac{|v|}{\lambda}}\right). \qquad (13c)$$

Fig. 2 shows plots of functions $L_i(v)$, given by Eqs. (13a)–(13c). One can see that the functions differ substantially from Lorentzian curves. A common feature is an infinite value of the first derivative at $v = 0$ (Fig. 3), which is due to the fact that $f_i(t)\underset{t\to\infty}{\sim}t^{-3/2}$. In this case ($T\to\infty$) the line width between the points of maximum slopes (peak-to-peak line width, Δv_{PP}) cannot be found. Still, the line may be characterized by its full width at half magnitude (fwhm), $\Delta v_{1/2}$; e.g., for $L_1(v)$

$$\Delta v_{1/2} = 2\lambda. \qquad (14)$$

As for the spectral wings ($v \gg \lambda$), for distribution (8a) $L_1(v)\underset{v\to\infty}{\sim}|v|^{-1/2}$ decays slower than the Lorentzian contour $|v|^{-2}$, for distribution (8b) – much faster, $L_2(v)\underset{v\to\infty}{\sim}\exp(-\sqrt{2|v|/\lambda})$, and for distribution (8c) – as fast as the Lorentzian contour.

The situation changes if a long ($T\gg\lambda^{-1}$), but finite time T is taken into account. In this case, the
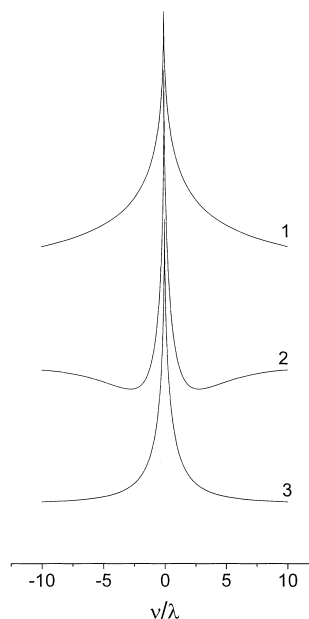

Fig. 2. Low-field MARY lines for different lifetime distribution functions ($1 - f_1(t)$, $2 - f_2(t)$ and $3 - f_3(t)$) when $1/T = 0$.
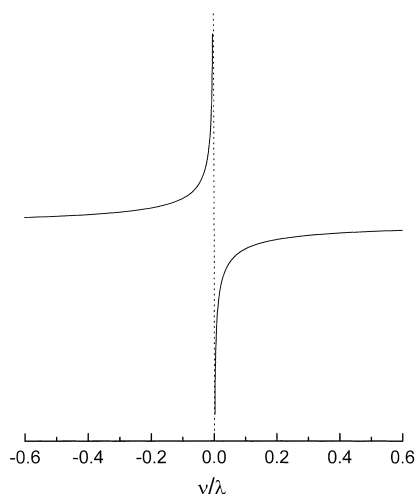
Fig. 3. First derivative of $L_1(v)$ when $1/T = 0$. Peak-to-peak width cannot be found since the first derivative is infinite in the vicinity of $v = 0$.

first derivatives of $L_i(v)$ are closer to the Lorentzian. Figs. 4 and 5 show plots of function $L_1(v)$ and its first derivative for several values of λT. It is now possible to determine the peak-to-peak width of $L_i(v)$. Analytical expressions can be easily derived when $\lambda T \gg 1$ and $vT \sim 1$

$$L_1(v) \approx 1 - \frac{1}{\sqrt{2\lambda T}}\sqrt{1 + \sqrt{1 + v^2 T^2}},$$

$$L_2(v) \approx 1 - \sqrt{\frac{2}{\lambda T}}\sqrt{1 + \sqrt{1 + v^2 T^2}}, \qquad (15)$$

$$L_3(v) \approx 1 - \sqrt{\frac{\pi}{2\lambda T}}\sqrt{1 + \sqrt{1 + v^2 T^2}},$$

which gives

$$\Delta v_{PP} = \frac{2\sqrt{3}}{T}. \qquad (16)$$

A remarkable feature of this formula is the fact that in this limiting case, the peak-to-peak width of the line is determined solely by the time T but not by the rate of the geminate recombination λ. Note that this width is three times the width of the equivalent Lorentzian contour corresponding to the decay time T,
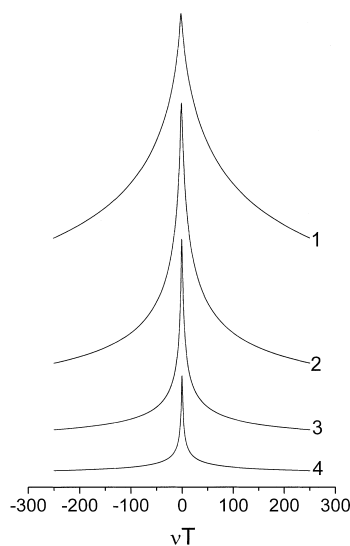

Fig. 4. Low-field MARY line $L_1(v)$ for different values of λT: 1 – $\lambda T = 100$, 2 – $\lambda T = 10$, 3 – $\lambda T = 1$, 4 – $\lambda T = 0.1$.
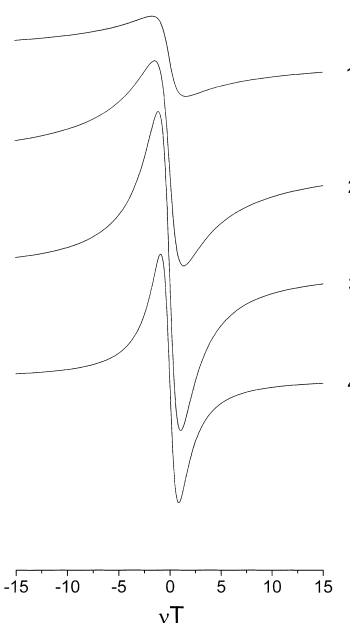

Fig. 5. First derivative of $L_1(v)$ for different values of λT: 1 – $\lambda T = 100$, 2 – $\lambda T = 10$, 3 – $\lambda T = 1$, 4 – $\lambda T = 0.1$.

$$\Delta v_{PP}^{L} = \frac{2}{\sqrt{3}}\frac{1}{T}. \qquad (17)$$

In other words, the geminate recombination does not contribute to the peak-to-peak width of

the low-field MARY line. It only scales (in the limit $\lambda T \gg 1$ by the factor of three) the line width that is determined by chemical transformations and spin relaxation. The specific value of the scaling factor is determined by the asymptotic behaviour of the model functions $f_i(t) \propto t^{-3/2}$ in the limit $t \to \infty$. For a more general asymptotic law $f(t) \propto t^{-n/2}$, for $4 > n > 2$, the following expression holds true:

$$\frac{\Delta v_{PP}}{\Delta v_{PP}^L} = \sqrt{3} tg \frac{\pi}{6-n}, \qquad (18)$$

giving $\Delta v_{PP}/\Delta v_{PP}^L = 3$ for $n = 3$.

It is necessary to note that the peak-to-peak width Δv_{PP} is considerably smaller than $\Delta v_{1/2}$ (see Eq. (14)): at $\lambda T \gg 1$, the points of maximum slope are located in the narrow region of the spectrum peak (see Fig. 4), i.e. in the vicinity of the frequencies satisfying the condition $vT \sim 1$ where expansions (15) are valid. Qualitatively, the spectral features in the vicinity of the peak (where $vT \ll 1$) are determined by the long-time behaviour of $f_{1,2,3}(t)$, which is the same for all the distributions.

In the opposite limit, $\lambda T \ll 1$,

$$L_1(v) \approx \sqrt{\frac{\lambda T}{2} \frac{(1 + \sqrt{1 + v^2 T^2})}{1 + v^2 T^2}}, \qquad (19a)$$

$$L_2(v) \sim \exp\left(-\sqrt{\frac{2}{\lambda T}}\right) \approx 0, \qquad (19b)$$

$$L_3(v) \approx \frac{\lambda T}{2(1 + v^2 T^2)}. \qquad (19c)$$

Although in this case the width of the spectrum line is determined by the exponential decay, the shape of $L_1(v)$ and $L_2(v)$ differs from the Lorentzian. For $L_1(v)$, the full width at half magnitude and the peak-to-peak width are

$$\Delta v_{1/2} \approx 5.09/T \quad \text{and} \quad \Delta v_{PP} \approx 1.45/T, \qquad (20)$$

respectively, while for a Lorentzian contour determined only by the exponential decay

$$\Delta v_{1/2}^L = 2/T \quad \text{and} \quad \Delta v_{PP}^L \approx 1.15/T. \qquad (21)$$

The deviation from the Lorentzian shape is associated with the divergence of the distribution $f_1(t)$ at $t \to \infty$. The absence of such a divergence for the distribution $f_3(t)$ results in the Lorentzian shape of the spectral line $L_3(v)$. For a more general asymptotic behaviour $f(t) \propto t^{-k}$ in the limit $t \to 0$ the following expression holds true:

$$\frac{\Delta v_{PP}}{\Delta v_{PP}^L} = \sqrt{3} tg \frac{\pi}{2(3-k)}, \quad k < 1. \qquad (22)$$

Eq. (22) gives the ratio of widths equal to 1 and 1.26 for $k = 0$ and $k = 1/2$, respectively, which is in agreement with Eqs. (20) and (21). Exponential vanishing of the distribution $f_2(t)$ at $t \to 0$ leads to the very low intensity of $L_2(v)$.

The dependencies of the ratio $\Delta v_{PP}/\Delta v_{PP}^L$ vs. λT are shown in Fig. 6. It is seen that the curves coincide at high values of λT. On the contrary, for small values of this parameter, the ratios $\Delta v_{PP}/\Delta v_{PP}^L$ differ for various pair recombination functions because of their different short-time behaviour.

The largest deviation of the lineshape from the Lorentzian can be seen in the second derivative of
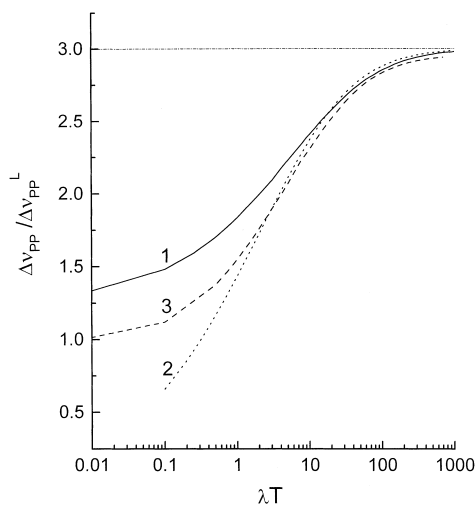

Fig. 6. Plot of the ratio $\Delta v_{PP}/\Delta v_{PP}^L$ of the peak-to-peak line width to the peak-to-peak line width of the purely Lorentzian contour vs. λT for different lifetime distribution functions: 1 – for $f_1(t)$, 2 – for $f_2(t)$, 3 – for $f_3(t)$.
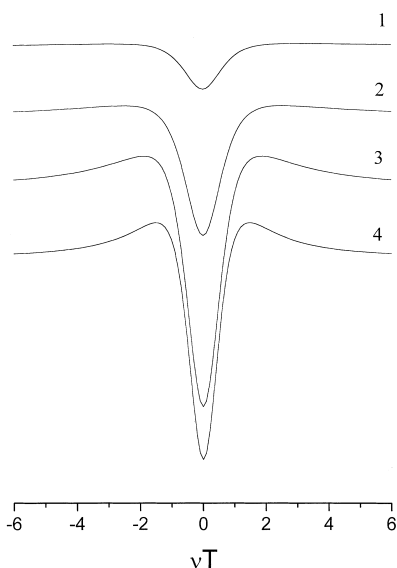
Fig. 7. Second derivatives of $L_1(v)$ for different values of λT: $1 - \lambda T = 100$, $2 - \lambda T = 10$, $3 - \lambda T = 1$, $4 - \lambda T = 0.1$. For convenience, the curves are shifted vertically.

Fig. 8. Absolute value of the ratio R of minimum and maximum on the second derivative vs. λT for different pair lifetime distribution functions: 1 – for $f_1(t)$, 2 – for $f_2(t)$, 3 – for $f_3(t)$.

$L_i(v)$ (Fig. 7). Consider the ratio R of the absolute minimum and maximum of the second derivative. For a Lorentzian line, this ratio is equal to 4. In Fig. 8 the ratio R is plotted as a function of λT. Fig. 9 shows the plot of the ratio $\Delta v_{PP}/\Delta v_{PP}^L$ vs. R. These two plots allow one to determine the two parameters of the model, the decay rate $1/T$ and the rate λ of the geminate recombination kinetics, from the experimentally determined values of R and Δv_{PP}. At large R values, this method is not sensitive to the form of the pair recombination kinetics.

3. Experimental evidence for non-Lorentzian shape

To find out how large the deviation is from the Lorentzian contour in a real system, we have analysed the shape of the MARY line in low magnetic fields recorded [15] for the pairs RH$^+$/C$_6$F$_6^-$ in irradiated linear alkanes, RH. In these pairs, the hyperfine coupling constant $A(6F) = 135$ G in the radical anion is fairly large, whereas the couplings in RH$^+$ is believed to be averaged out by charge exchange with the solvent molecules.
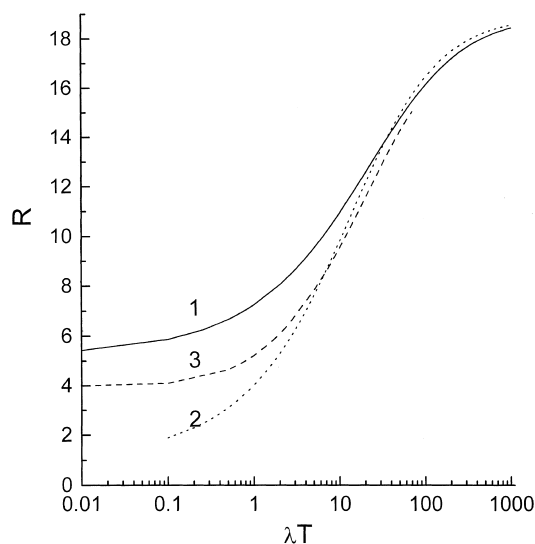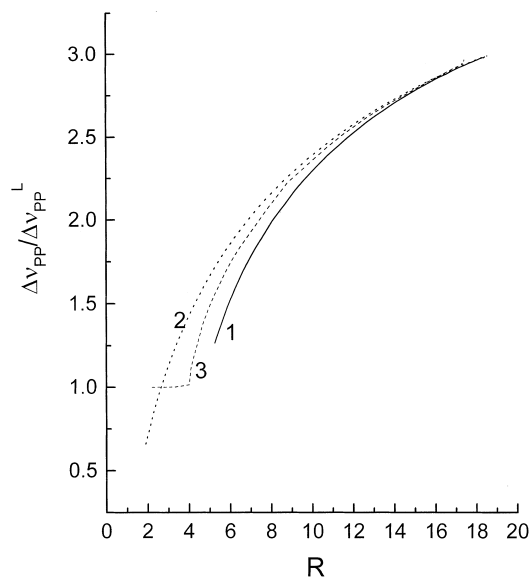

Fig. 9. Plot of the ratio $\Delta v_{PP}/\Delta v_{PP}^L$ vs. R for different pair lifetime distribution functions: 1 – for $f_1(t)$, 2 – for $f_2(t)$, 3 – for $f_3(t)$.

Our examination shows that the wings of the low-field lines, recorded as the first derivative using field modulation technique, decay slower as compared to the Lorentzian line. The deviation from

the Lorentzian is more apparent when the spectrum is presented as the second derivative and the ratio R is measured.

The ratios R for C_8, C_{10}, C_{12} and C_{16} n-alkanes are listed in Table 1. The R values were obtained in two different ways: by approximation of the first derivative fragments by a cubic polynom with the subsequent determination of maximum slopes, and by smoothing of the first derivative as described in Ref. [19] with the subsequent differentiation of the smoothed curves. In some cases, the lines were directly recorded at the second harmonic of the reference frequency. The results obtained in different ways agree within ± 0.5.

In all of these pairs the ratio R significantly exceeds the value $R_L = 4$ that corresponds to the Lorentzian line. In principle, the shape of the line can be affected by the multifrequency of spin dynamics for the pair with six spin-1/2 nuclei (see Eq. (5)) and the violation of the "isolated line" condition. The former factor tends to increase R. However, our estimates show that it cannot provide the observed values of $R = 6$–7. As computer simulations show, the latter factor, on the contrary, decreases the ratio R. Thus, the observed high values of $R = 6$–7 must be due to nonexponential kinetics.

Fig. 10 shows an example of describing an observed low-field MARY line by the presented theory. The figure gives the experimental line for 0.012 M solution of hexafluorobenzene in decane at room temperature. The observed peak-to-peak width of the line ΔH_{PP} is approximately 19 G, and the ratio R equals approximately 6.25 (Table 1). For the function $f_3(t)$ from Fig. 9, we obtain $\Delta v_{PP}/\Delta v_{PP}^L = 1.8$ which gives $\Delta v_{PP}^L = 10.6$ G and $T = 6.2$ ns. From Fig. 8, we obtain $\lambda T = 2$, giving $\lambda = 3.2 \times 10^8\ s^{-1}$. The smooth solid curves in Fig. 10 show the first and second derivatives of the line calculated for the function $f_3(t)$ using the found values of λ and T. The agreement between the observed and calculated lines is very satisfactory. The dashed curves show how a Lorentzian line with the same time $T = 6.2$ ns looks like. Apparently, the actually observed line is wider, and its wings fall off less rapidly than for the Lorentzian one. And as has already been stated, the observed line cannot be described by just varying the width of the Lorentzian contour.
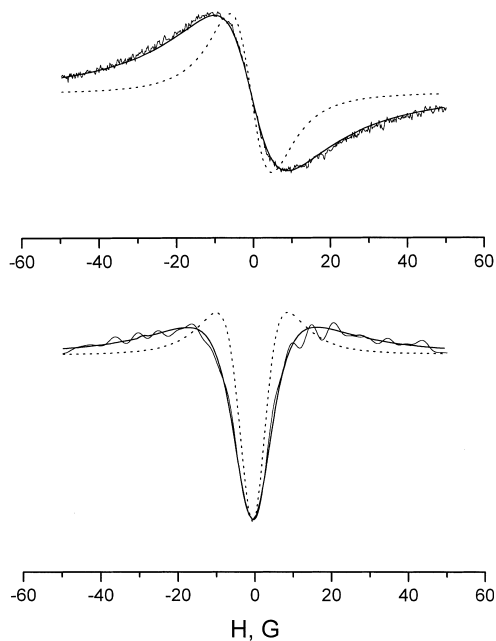
Table 1
The ratio R of the extrema on the second derivative of the low-field MARY lines for $(n$-alkane$)^+/($hexafluorobenzene$)^-$ pairs in X-ray-irradiated alkane solutions of 1.2×10^{-2} M hexafluorobenzene at room temperature

Alkane	η	ΔH_{pp} [15]	R^a	R^b
C_8H_{18}	0.54	25	6.5	7.6
$C_{10}H_{22}$	0.92	15	6.3	6.2
$C_{12}H_{26}$	1.35	12	5.8	6.2
$C_{16}H_{34}$	3.34	7	7.4	6.5

η is the viscosity of the alkane at room temperature, cP; ΔH_{PP} is the width of the low-field MARY line measured between the points of maximum slope (extrapolated to zero concentration of hexafluobenzene, see Ref. [15]), G.
[a] The ratio obtained by polynomial approximation.
[b] The ratio obtained by smoothing and subsequent differentiation (see text for details).

Fig. 10. Low-field MARY line for 1.2×10^{-2} M solution of C_6F_6 in decane recorded as a first derivative (top) and the result of its numerical differentiation (bottom). The smooth solid curves show simulation for function f_3. The dashed curves show the Lorentzian contour calculated for the same value of parameter T that was used for simulation (refer to text for details).

Similar calculations for functions $f_1(t)$ and $f_2(t)$ give the second derivatives curves that are virtually identical to the calculated curve from Fig. 10. The curves for the first derivatives differ a little bit at the wings of the line, which fall off slightly steeply for $f_2(t)$ and slightly less rapidly for $f_1(t)$, but this difference is well within the limits of the noise level of the experimental line. We can conclude that under our conditions, the shape of the line is not sensitive to the choice of model functions and is mostly determined by their long-time behaviour.

The values of R do not change within the limits of experimental accuracy for holes of different alkanes. This result seems to contradict the observed trends in the line width which indicate a systematic increase of the lifetime T of the spin-correlated pairs $RH^+/C_6F_6^-$ with the carbon number of the alkane RH. However, it must be taken into account that the parameter λ decreases with the lengthening of the carbon chain due to increase in viscosity. Probably, these two trends compensate each other and the value λT does not change much from one alkane to another.

4. Conclusions

Our examination shows that nonexponential character of the geminate pair recombination can lead to non-Lorentzian shape of low-field MARY line. The deviation from the Lorentzian shape is most clear when the times of spin relaxation and chemical decay are much longer than the characteristic time of the geminate recombination. In this case, the line shape is determined primarily by the long-time behaviour of the recombination kinetics and is less sensitive to its behaviour at short times. As compared to the Lorentzian spectrum, the low-field MARY line has broader wings and a sharper peak so that its fwhm is much larger than the peak-to-peak separation. We found that the fwhm is primarily related to the characteristic recombination time, while the peak-to-peak distance reflects the times of spin relaxation and chemical decay. In this case, the contribution of the decay processes to the width between the points of maximum slope noticeably (up to three times in the limit of slow decay) exceeds that for the ex-

ponential kinetics. The analysis of experimental spectra for the pairs (n-alkane)$^+$/(hexafluorobenzene)$^-$ demonstrates that the shape of the low-field MARY lines is indeed not Lorentzian and is well described by the suggested theory.

References

[1] O.A. Anisimov, V.M. Grigoryants, S.V. Kiyanov, K.M. Salikhov, Yu.N. Molin, Teor. Eksper. Khim. 18 (1982) 292 (in Russian).
[2] H. Fischer, Chem. Phys. Lett. 100 (1982) 255.
[3] C.A. Hamilton, J.P. Hewitt, K.A. McLauchlan, U.E. Steiner, Molec. Phys. 65 (1988) 423.
[4] I.A. Shkrob, V.F. Tarasov, A.L. Buchachenko, Chem. Phys. 153 (1991) 443.
[5] S.N. Batchelor, C.W. Kay, K.A. McLauchlan, I.A. Shkrob, J. Phys. Chem. 97 (1993) 13250.
[6] D.V. Stass, N.N. Lukzen, B.M. Tadjikov, Yu.N. Molin, Chem. Phys. Lett. 233 (1995) 444.
[7] U. Till, C.R. Timmel, B. Brocklehurst, P.J. Hore, Chem. Phys. Lett. 298 (1998) 7.
[8] D.V. Stass, B.M. Tadjikov, Yu.N. Molin, Chem. Phys. Lett. 235 (1995) 511.
[9] V.O. Saik, A.E. Ostafin, S. Lipsky, J. Chem. Phys. 103 (1996) 7347.
[10] V.O. Saik, A.E. Ostafin, S. Lipsky, J. Chem. Phys. 104 (1996) 319.
[11] V.M. Grigoryants, S.D. McGrane, S. Lipsky, J. Chem. Phys. 109 (1998) 7354.
[12] V.O. Saik, S. Lipsky, Chem. Phys. Lett. 264 (1997) 649.
[13] B. Broklehurst, Molec. Phys. 96 (1999) 2283.
[14] D.V. Stass, N.N. Lukzen, B.M. Tadjikov, V.M. Grigoryants, Yu.N. Molin, Chem. Phys. Lett. 243 (1995) 533.
[15] K.M. Salikhov, Yu.N. Molin, R.Z. Sagdeev, A.L. Buchachenko, Spin Polarization and Magnetic Effects in Radical Reactions, Elsevier, Amsterdam, 1984.

[16] F.B. Sviridenko, D.V. Stass, Yu.N. Molin, Chem. Phys.
     Lett. 297 (1998) 343.
[17] V.A. Bagryansky, O.M. Usov, N.N. Lukzen, Yu.N. Molin,
     Appl. Magn. Reson. 12 (1997) 505.

[18] S.F. Rzad, P.P. Infelta, J.M. Warman, R.H. Schuler, J.
     Chem. Phys. 52 (1970) 3971.
[19] Yu. Ya. Efimov, Vibr. Spectr., accepted.